Electronic Supplementary Information for:

Effect of polyelectrolyte interdiffusion on the electron transport in electro-active polyelectrolyte multilayers

Raphael Zahn,* Géraldine Coullerez, János Vörös and Tomaso Zambelli

Laboratory of Biosensors and Bioelectronics, Institute for Biomedical Engineering, ETH Zürich, Switzerland.

* To whom correspondence should be addressed.

e-mail: zahn@biomed.ee.ethz.ch

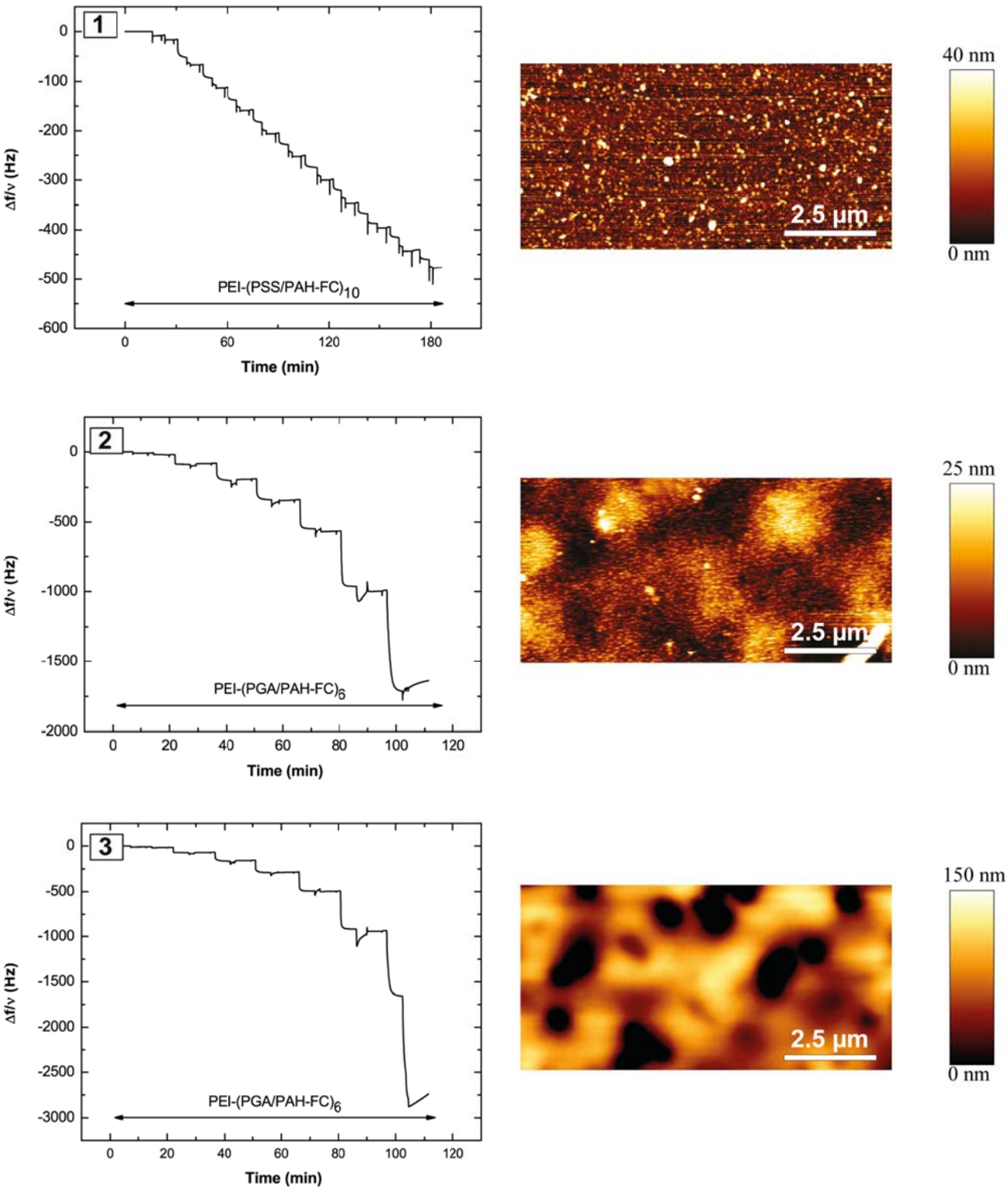

Fig. S1 QCM-D data (left side) and AFM data (right side) showing the buildup and the surface topology of (1) PEI-(PSS/PAH-FC)$_{10}$, (2) un-crosslinked PEI-(PGA/PAH-FC)$_6$ and (3) crosslinked PEI-(PGA/PAH-FC)$_6$.

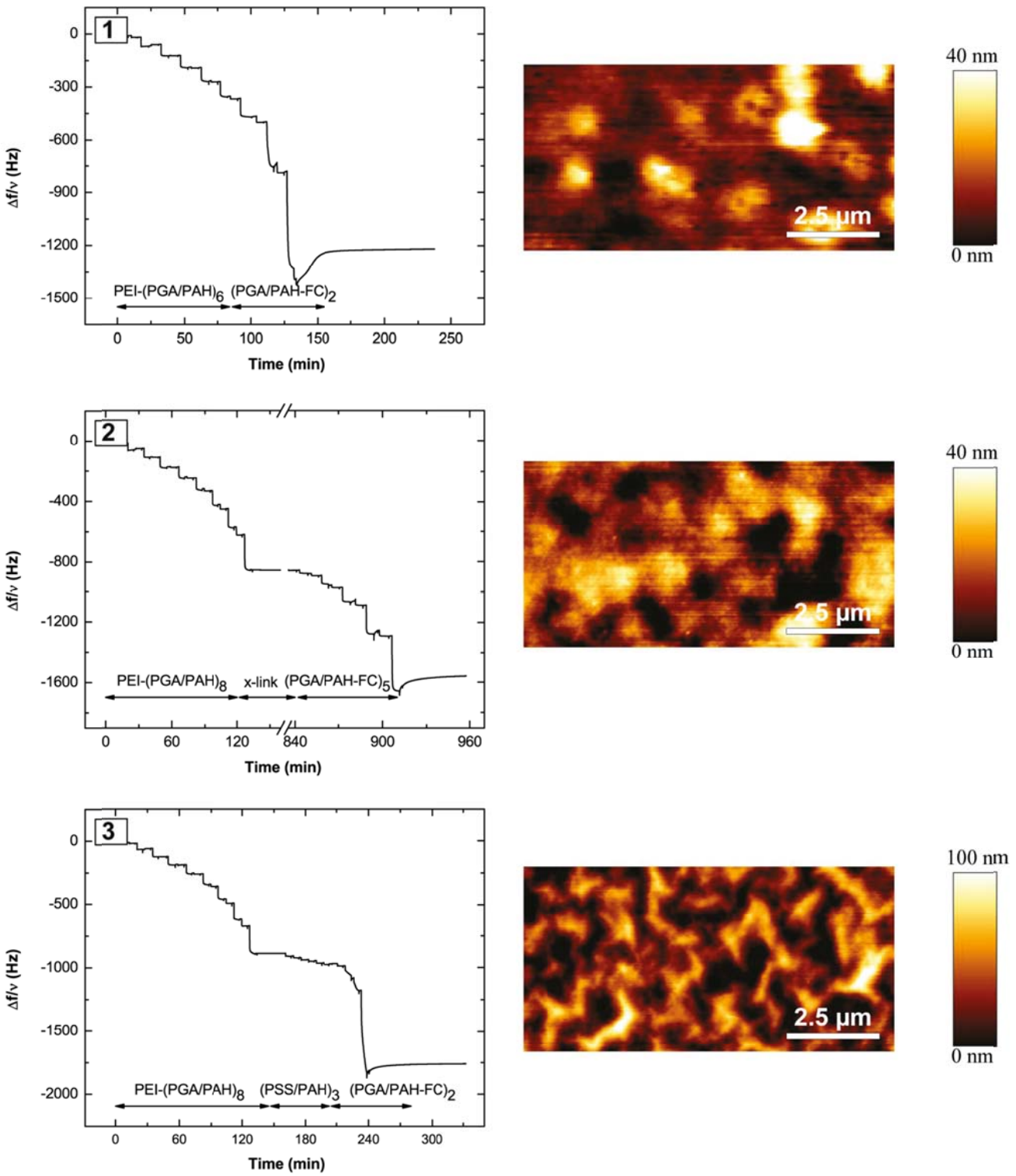

Fig. S2 QCM-D data (left side) and AFM data (right side) showing the buildup and the surface topology of (1) PEI-(PGA/PAH)$_6$-(PGA/PAH-FC)$_2$, (2) PEI-(PGA/PAH)$_8$-xlink-(PGA/PAH-FC)$_5$, and (3) PEI-(PGA/PAH)$_8$-(PSS/PAH)$_3$-(PGA/PAH-FC)$_2$.

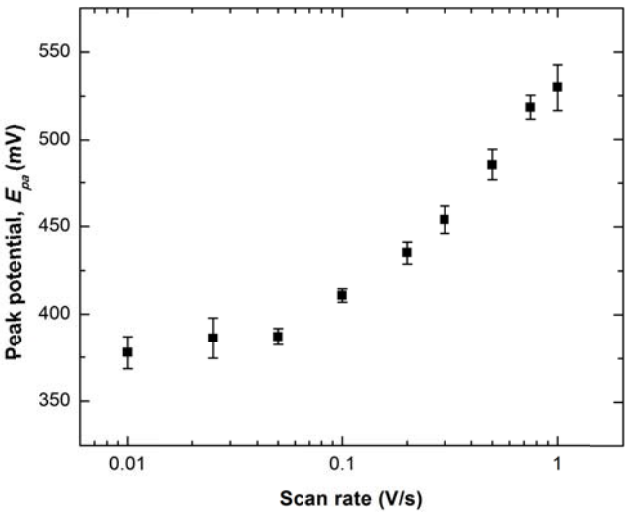

Fig. S3 Anodic peak potentials, E_{pa}, of cyclic voltammograms at various scan rates for PEI-(PGA/PAH-FC)$_6$. See Fig. 1.1 in the main article for the voltammograms.

Characterization of the multilayer assembly by QCM-D and AFM

Fig. S1 shows the buildup (by QCM-D; left side) and the surface topology (by AFM; right side) of: (1) PEI-(PSS/PAH-FC)$_{10}$, (2) un-crosslinked PEI-(PGA/PAH-FC)$_6$ and (3) crosslinked PEI-(PGA/PAH-FC)$_6$. The electrochemical characterization of these multilayer systems by cyclic voltammetry is shown in Fig. 1 in the main article. The QCM-D data shows linear growth for PSS/PAH-FC multilayers and exponential growth for PGA/PAH-FC multilayers. This is in agreement with literature on these multilayer systems.[1, 2] The exponential growth of PGA/PAH-FC depends strongly on the initial condition. Therefore, the final frequency shift for the buildup of PEI-(PGA/PAH-FC)$_8$ multilayers varies between 1700 Hz (see Fig. 2.2) and 2700 Hz (see Fig. 2.3).

The surface topology appears smooth for the non-crosslinked films (see Fig. 1.1, Fig. 1.2) and slightly rougher for the crosslinked films (see Fig. 1.3).

Fig. S2 shows the buildup and the surface topology of: (1) PEI-(PGA/PAH)$_6$-(PGA/PAH-FC)$_2$, (2) PEI-(PGA/PAH)$_8$-xlink-(PGA/PAH-FC)$_5$, and (3) PEI-(PGA/PAH)$_8$-(PSS/PAH)$_3$-(PGA/PAH-FC)$_2$. A scheme, which illustrates electron transfer and polymer interdiffusion in these systems, is shown in the main article (Scheme 2). Electrochemical characterization by cyclic voltammetry is shown in Fig. S4. The QCM-D data shows exponential growth for the PEI-(PGA/PAH)$_6$-(PGA/PAH-FC)$_2$ multilayer (see Fig. S2.1). The multilayer grows at the same rate for both blocks - the one containing PAH and the one containing electrochemically active PAH-FC. This behavior shows that the use of the chemically modified PAH-FC does not alter the interdiffusion properties of the polyelectrolytes in PGA/PAH multilayers. However, this is no longer the case if the PGA/PAH multilayer is crosslinked. Fig. S2.2 shows the adsorption of a crosslinked PEI-(PGA/PAH)$_8$ block, followed by the deposition of a native (non-crosslinked) (PGA/PAH-FC)$_5$ block. The frequency shifts in the QCM-D data show that the exponential growth does not continue with the same rate after the crosslinking, but restarts at a new rate. This indicates that the crosslinked multilayer largely blocks the interdiffusion of the polyelectrolytes. A similar effect is obtained if a PSS/PAH block is inserted between a PGA/PAH block and a PGA/PAH-FC block (see Fig. S2.3). In this case, the PSS/PAH layers hinder the interdiffusion of polyelectrolytes from one PGA/PAH block to the other one.[2] This results in two different growth rates for the PGA/PAH and the PGA/PAH-FC block, respectively.

The AFM images show smooth layers for PEI-(PGA/PAH)$_6$-(PGA/PAH-FC)$_2$ and PEI-(PGA/PAH)$_8$-xlink-(PGA/PAH-FC)$_5$ (Fig. S2.1, Fig. S2.2), while the surface the PEI-(PGA/PAH)$_8$-(PSS/PAH)$_3$-(PGA/PAH-FC)$_2$ multilayers is slightly rougher (Fig. S2.3).

Electrochemical characterization

Fig. S3 shows the anodic peak potentials, E_{pa}, of cyclic voltammograms at various scan rates for PEI-(PGA/PAH-FC)$_6$. E_{pa} shifts to more negative values with increasing scan rates. This indicates that the voltammetric responses are of quasireversible nature. Fig. S4 shows the electrochemical characterization for: (1) PEI-(PGA/PAH)$_6$-(PGA/PAH-FC)$_2$, (2) PEI-(PGA/PAH)$_8$-xlink-(PGA/PAH-FC)$_5$, and (3) PEI-(PGA/PAH)$_8$-(PSS/PAH)$_3$-(PGA/PAH-FC)$_2$. On the left side, the cyclic voltammograms for various scanning speeds are shown. The anodic peak currents i_{pa} were obtained from these voltammograms after subtracting the background charging current. The right side shows Randles-Sevcik $i_{pa}/\sqrt{v}$ plots, which were used to determine the electron diffusion coefficients D_E according to Eq. (1). A table of the obtained electron diffusion coefficients can be found in in the main article (Table 1).

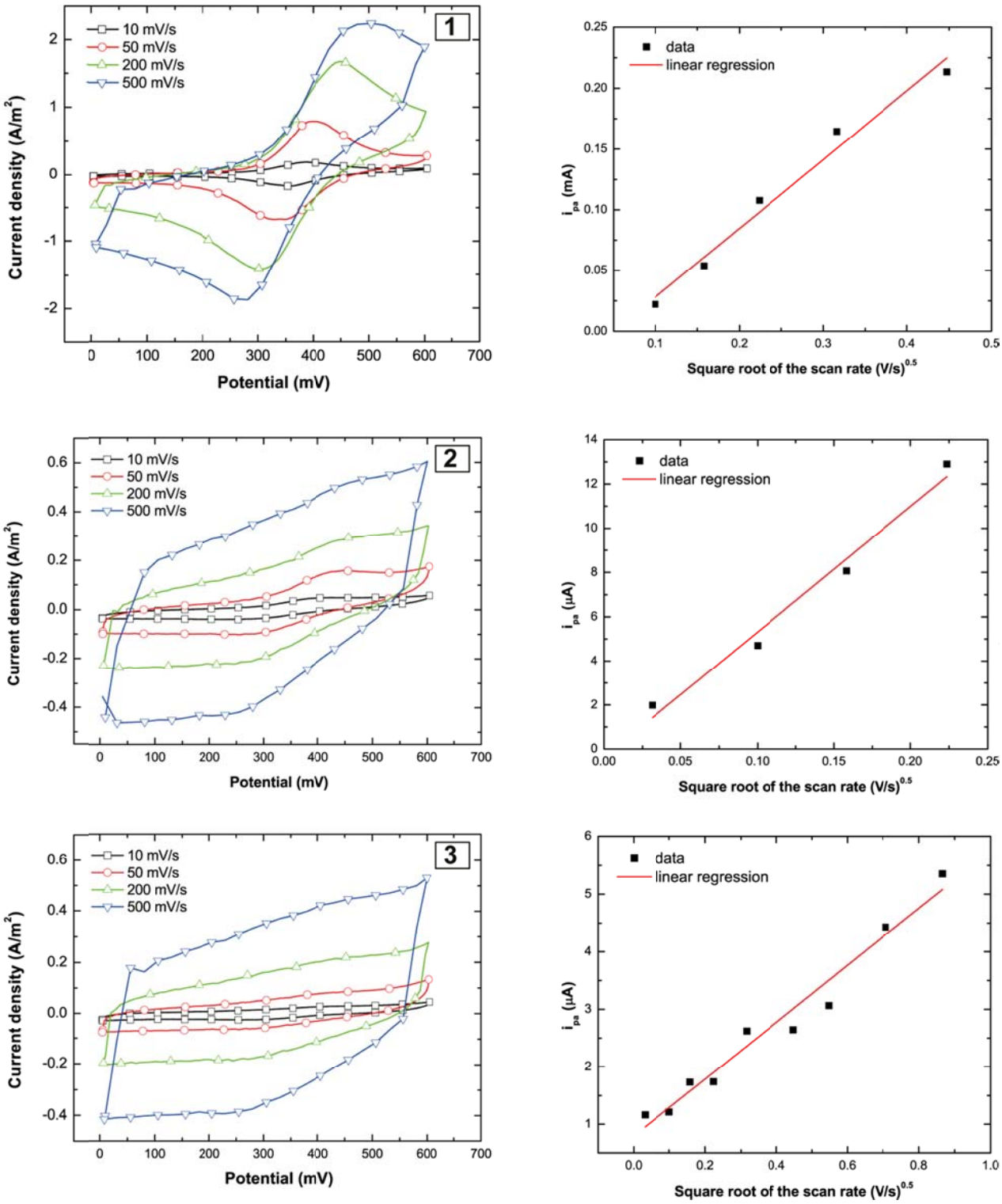

Fig. S4 Cyclic voltammograms at various scanning speeds (left side) and Randles-Sevcik $i_{pa}/\sqrt{v}$ plots (right side) for (1) PEI-(PGA/PAH)$_6$-(PGA/PAH-FC)$_2$, (2) PEI-(PGA/PAH)$_8$-xlink-(PGA/PAH-FC)$_5$, and (3) PEI-(PGA/PAH)$_8$-(PSS/PAH)$_3$-(PGA/PAH-FC)$_2$.

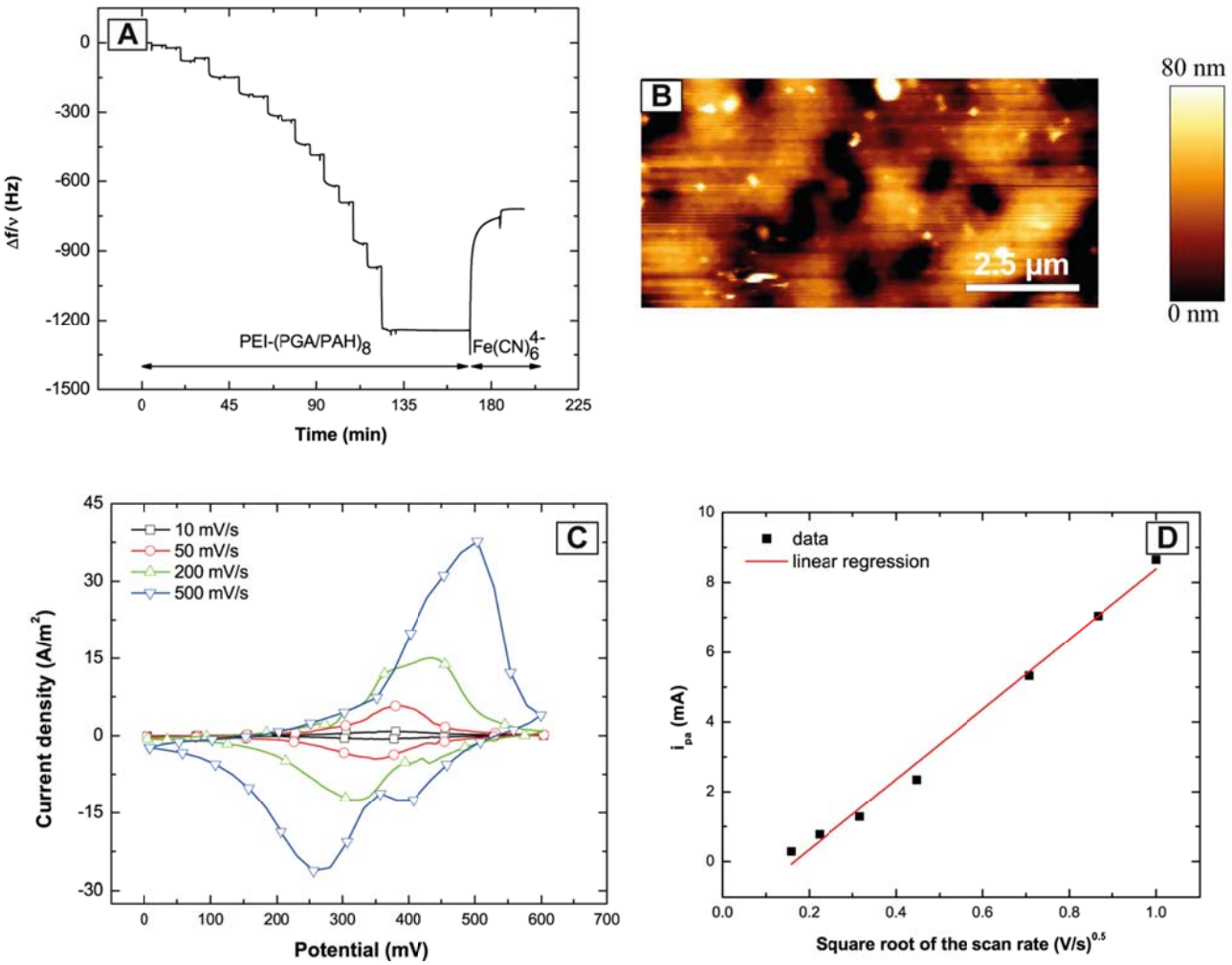

Fig. S5 Characterization of ferrocyanide-containing PEI-(PGA/PAH)$_8$ multilayers. (A) QCM-D data showing the multilayer buildup and the ferrocyanide uptake. (B) AFM micrograph showing the surface topology. (C) Cyclic voltammograms at various scanning speeds. (C) Randles-Sevcik $i_{pa}/\sqrt{v}$ plots.

Characterization of PGA/PAH multilayers containing ferrocyanide

Fig. S5 shows the characterization of ferrocyanide-containing PGA/PAH multilayers by (A) QCM-D, (B) AFM and (C, D) cyclic voltammetry. The QCM-D data shows the exponential growth of a PEI-(PGA/PAH)$_8$ multilayer. Upon addition of ferrocyanide, the frequency in the QCM-D measurement increased by about 1/3 of the frequency shift measured for the multilayer buildup (see Fig. S4A). This contraction of the multilayer is due to a replacement of PGA-polyelectrolyte by smaller ferrocyanide ions.[3]

The surface topology of the PGA/PAH multilayers containing ferrocyanide is slightly rougher (see Fig. S5B) compared to the PGA/PAH multilayers without ferrocyanide (see Fig. S1.2).

We used cyclic voltammetry to investigate the electron-transport mechanism in PGA/PAH multilayers containing ferrocyanide. Fig. S5C shows voltammograms for various scanning speeds.

The return scans of the voltammograms recorded at scanning rates above 100 mV/s show partial or complete double peaks. This peak splitting can be explained by a distribution of the Donnan potentials of the ferrocyanide ions in the multilayer. This behavior has been previously been described for a physicochemically very similar multilayer systems (Hyaluronic acid/Poly(allylamine hydrochloride) containing ferrocyanide).[4] Fig. S5D shows Randles-Sevcik $i_{pa}/\sqrt{v}$ plots, which were used to determine the electron diffusion coefficients according to Eq. (1) (see also Table 1 in the main article).

References

1. P. Lavalle, C. Gergely, F. J. G. Cuisinier, G. Decher, P. Schaaf, J. C. Voegel and C. Picart, *Macromolecules*, 2002, **35**, 4458-4465.
2. F. Boulmedais, M. Bozonnet, P. Schwinte, J. C. Voegel and P. Schaaf, *Langmuir*, 2003, **19**, 9873-9882.
3. R. Zahn, F. Boulmedais, J. Voros, P. Schaaf and T. Zambelli, *The journal of physical chemistry. B*, 2010, **114**, 3759-3768.
4. C. Betscha and V. Ball, *Soft Matter*, 2011, **7**, 1819.